

## DAMPING CHARACTERISTICS OF A MICROMACHINED PIEZOELECTRIC DIAPHRAGM-BASED PRESSURE SENSOR FOR UNDERWATER APPLICATIONS

*C.W. Tan<sup>1,2</sup>, A.G.P. Kottapalli<sup>2</sup>, Z.H. Wang<sup>2</sup>, X. Ji<sup>2</sup>, J.M. Miao<sup>2\*</sup>, G. Barbastathis<sup>1,3</sup> and M. Triantafyllou<sup>1,3</sup>*

<sup>1</sup>Center for Environmental Sensing and Modeling, SMART Centre, SINGAPORE

<sup>2</sup>School of Mechanical and Aerospace Engineering, Nanyang Technological University, SINGAPORE

<sup>3</sup>Department of Mechanical Engineering, Massachusetts Institute of Technology, MA, USA

### ABSTRACT

This paper reports on the underwater damping characteristics of a micromachined piezoelectric pressure sensor packaged using liquid crystal polymer (LCP) and polydimethylsiloxane (PDMS). In water, its sensitivity is flat about 6 dB (ref. 1 V/Pa) from 20 to 400 Hz while its bandwidth is 1.2 kHz. In air, its sensitivity is about -33 dB (ref. 1 V/Pa) at low frequency and increases significantly after 4 kHz. The damped response in water can be attributed to the introduction of additional mass and damping elements to the sensor structure, which reduces the quality factor of the diaphragm. The larger sensitivity in water is due to higher pressure as a result of the denser water environment.

### KEYWORDS

Microfabrication, damping, piezoelectric sensor, LCP, underwater packaging.

### INTRODUCTION

Microelectromechanical system (MEMS) devices are in demand worldwide due to their miniaturized size, better performance, low cost and ease of fabrication. Despite the size advantage, one major challenge emerges during the design of such devices, which involves the damping characteristics of both the mechanical structures and the deployment environments. If the damping characteristics are not optimized meticulously, one undesired consequence is the reduction of the bandwidth.

Previously, we have demonstrated that the introduction or the deficiency of viscous damping in mechanical structures can be utilized to tune the performance of MEMS devices desirably. It is demonstrated, via a PZT/Si diaphragm-based acoustic transducer, that its frequency response can be optimized by attaching a Si backplate with optimized slots and holes to introduce damping in the air gap, slots and holes [1, 2]. For the radio frequency (RF) MEMS shunt switch, an optimized air gap and strategically-positioned holes in the base substrate greatly enhance its switching speed, which can be attributed to the significant reduction of squeeze-film damping due to the perforated holes [3].

We have also demonstrated that the dynamic behaviour of the piezoelectric circular microdiaphragm sensor, either working in atmospheric surrounding or in aqueous environment, is strongly influenced by the medium damping [4]. The resonant frequency of the diaphragm decreases from vacuum to atmospheric condition due to an added mass effect while its quality factor experiences a drop from air to ethanol.

One major advantage of the single-crystal bulk piezoelectric plate is its excellent piezoelectric properties, which are superior to those of thin and thick films [5]. For example, a low leakage current permits a low cutoff frequency (typically, several GΩ and nF) in the frequency response, which enables very low-frequency signal to be measured. While the lower limit of the bandwidth is restricted by the electrical characteristics, the upper limit is dependent on the mechanical damping characteristics.

In this paper, the underwater damping characteristics of a piezoelectric sensor, packaged using LCP and PDMS, are described. Fabrication, modeling and underwater characterization results are also presented.

### FABRICATION

The key fabrication steps for the piezoelectric sensor include a low-temperature bonding technique using a spin-on polymer (Cytop) [6], integration of the PZT layer on the silicon substrate, formation of electrode interconnect and pads, chemical mechanical polishing (CMP) to thin down the bulk PZT plate, wet etching of the PZT layer [7] and releasing the diaphragm structure by using the deep reactive ion etching (DRIE) technique.

Figure 1 illustrates the fabrication sequence [2] of the piezoelectric sensor. Firstly, a Cr (10 nm)/Au (300 nm) electrode layer is sputtered on the device layer (20 μm) of a 4-inch SOI wafer and one side of a 90-mm PZT plate (300 μm). These metallic layers form the bottom electrode of the PZT/Si diaphragm. A layer of the Cytop polymer is spin-coated and patterned on the SOI wafer. The through-hole in the Cytop polymer layer is then filled by sputtering another layer of Cr (10 nm)/Au (300 nm) for the purpose of electrical interconnection (Fig. 1(a)). Secondly, the SOI wafer and the bulk PZT plate are bonded together thermally at 160 °C at a pressure of 3 bar for 30 min (Fig. 1(b)). Thirdly, the thick bulk PZT plate is thinned down to a thickness of about 27 μm using CMP (Fig. 1(c)). In the fourth step, a layer of Cr (10 nm)/Au (300 nm) is sputtered on the PZT layer to form the top electrode layer. The wet etching of PZT is performed alternatively in diluted HCl:HF and HNO<sub>3</sub> solutions with a photoresist mask to open a window to access the bottom electrode (not illustrated in Fig. 1(d)). After that, the backside handle layer (450 μm) of the SOI wafer is etched using DRIE until the embedded SiO<sub>2</sub> etch-stop layer to release the PZT/Si diaphragm (an ellipse with major and minor diameters of 6 mm and 4 mm, respectively) (Fig. 1(d)). Finally, the device wafer is then diced to release the individual sensor (8 x 8 mm<sup>2</sup>) (Inset of Fig. 2).

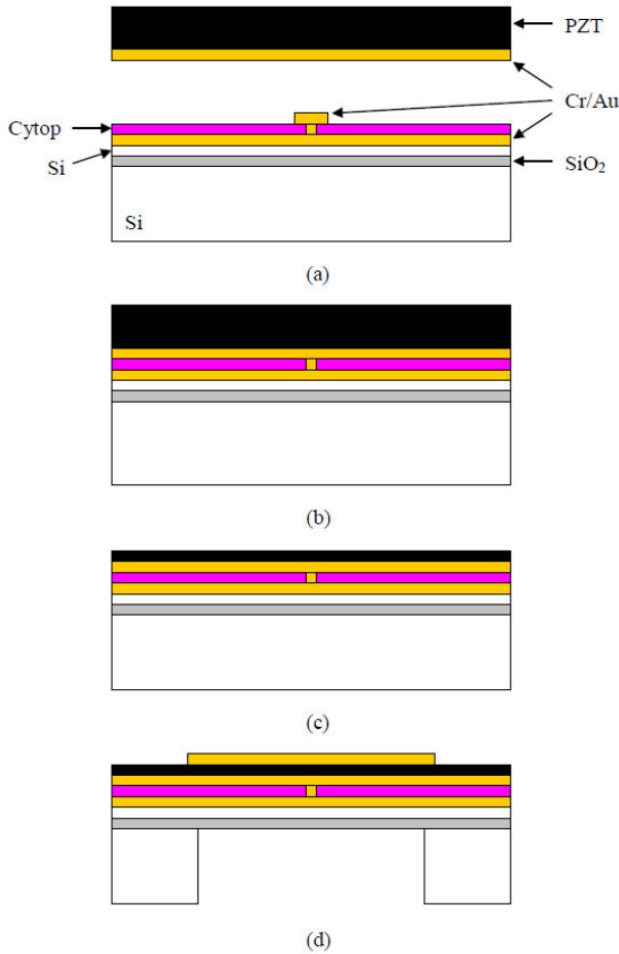


Figure 1: Fabrication sequence of the piezoelectric sensor: (a) Sputtering of Cr/Au on both PZT plate and SOI wafer, (b) thermal polymer bonding of PZT plate and SOI wafer, (c) thinning of PZT plate by using CMP and (d) sputtering of top Cr/Au electrode on the PZT layer and deep etching on the backside of SOI wafer to release the diaphragm.

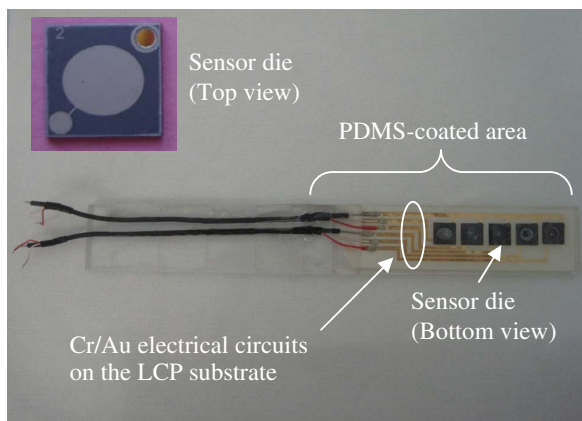


Figure 2: Underwater packaging scheme of the piezoelectric sensor.

For the underwater packaging scheme (Fig. 2), a LCP substrate [8] is used, on which Cr (10 nm)/Au (300 nm) electrical circuits are sputtered so that electrical connection via wires can be established with the bonded

sensors. Advantages of LCP include extremely low moisture absorption, superior hermetic sealing and excellent chemical resistance. Thus, it is able to maintain stable electrical, mechanical and dimensional properties in wet humid environments. For waterproofing and sealing purposes, PDMS is dispensed over the LCP substrate while avoiding the diaphragm openings.

## THEORETICAL CONSIDERATION

It is well-known that the vibration of an elastic diaphragm in a fluid is followed by the emission of acoustic radiation. The vibrating diaphragm sets the surrounding fluid into motion and the fluid produces a reactive effect in the form of added mass and damping forces on the vibrating diaphragm. The additional mass acts by lowering the resonant frequency of the diaphragm from the value as measured in air while the damping of the diaphragm will be increased. Lamb proposed a theoretical model that provides an estimate of the shift of the resonant frequency from vacuum to fluid (considering the fluid is incompressible). The resonant frequency in water can be approximated using Lamb's formula [9]

$$f_f = \frac{f_{vac}}{\sqrt{1+\beta}} \quad (1)$$

$$\beta = 0.6689 \frac{\rho_f a}{\rho_p h} \quad (2)$$

where  $f_f$  and  $f_{vac}$  are resonant frequencies in water and air, respectively,  $\rho_f$  and  $\rho_p$  are densities of water and plate, respectively,  $a$  is the plate radius and  $h$  is the plate thickness.

## CHARACTERIZATION

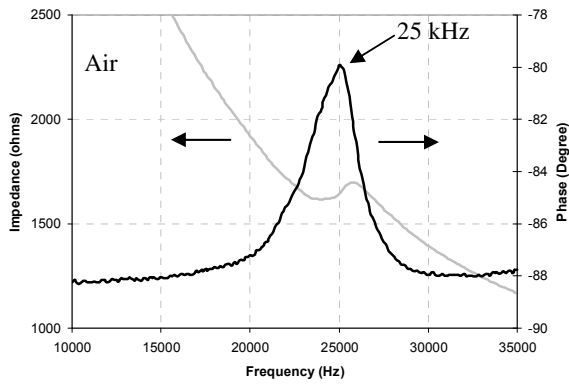
### Impedance Spectrum

Figure 3 illustrates the impedance spectra of the piezoelectric sensor characterized by Agilent 4294A Precision Impedance Analyzer in air and water. In Fig. 3(a), there is an occurrence of a well-defined resonance around 25 kHz when the measurement is performed in air. However, when the measurement is carried out in water (Fig. 3(b)), the resonant frequency reduces slightly to 23.3 kHz while its peak decreases significantly. When the measurement is performed in water, it introduces additional mass and damping elements to the sensor structure and reduces the quality factor of its diaphragm.

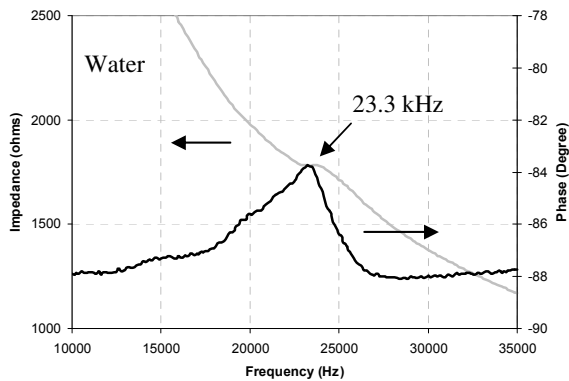
The calculated resonant frequency in water using Lamb's formula is about 19.7 kHz. The variance between the experimentally observed value and the theoretically calculated one is due to the following reasons. Firstly, Lamb's model does not account for the viscosity of the liquid medium. Secondly, the piezoelectric diaphragm used is a multilayered structure (comprising of Si, SiO<sub>2</sub>, Cytop and PZT). Moreover, we consider the resonant frequency in air and vacuum to be identical.

### Frequency Response

Figure 4 illustrates an underwater experimental setup



(a)



(b)

Figure 3: Impedance spectra of the piezoelectric sensor: (a) Air and (b) water.

to characterize the frequency response of the piezoelectric sensor. In this measurement setup, after the water tank is filled up with de-ionized (DI) water, a calibrated hydrophone (Aquarian Audio Products H2a hydrophone), which is able to detect underwater sound pressure from below 20 Hz to over 100 kHz, and the piezoelectric sensor (labeled device under test (DUT)) are placed next to each other in the tank and are driven by an underwater speaker (AQ339 Aquasonic® underwater loudspeaker from Clark Synthesis, Inc.), which has a frequency response from 20 Hz to 17 kHz. The gain of the power amplifier (B&K Power Amplifier Type 2706) for the underwater speaker is set to unity, the gain of the preamplifier (Aquarian Audio Products UPA-1 preamplifier) for the hydrophone is set to 60 dB (when it is used in conjunction with the H2a hydrophone, approximately 8 dB gain is added through the hydrophone buffer amplifier for a total of 60 dB) and the gain of the preamplifier (SRS SR560 Low-noise Preamplifier) for the sensor is set to 10.

To measure the frequency response of the sensor, Agilent 35670A Dynamic Signal Analyzer is used to provide a sweeping sinusoidal signal from 20 Hz to 40 kHz to drive the underwater speaker and simultaneously measure the output signals from both the hydrophone and sensor. Figure 5 illustrates the underwater frequency response plot of the piezoelectric sensor. As illustrated, the sensor provides a damped response with a flat

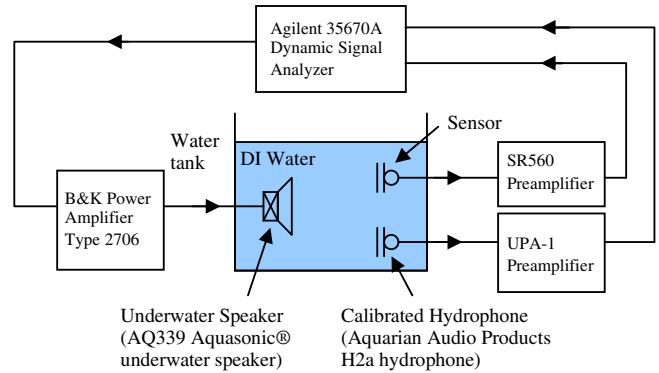


Figure 4: An underwater experimental setup.

sensitivity of about 6 dB (ref. 1 V/Pa) from 20 to 400 Hz while its bandwidth ( $\pm 3$  dB) is about 1.2 kHz.

In order to make comparisons between the underwater frequency response with that in air, the whole experimental setup of Fig. 4 is transferred to a sound-proof acoustic box for characterization in air. As illustrated in Fig. 5, in air, the sensor provides an underdamped response with a sensitivity of about -33 dB (ref. 1 V/Pa) at low frequency while its sensitivity increases significantly after 4 kHz. As pointed out earlier, the damped response observed in water can be attributed to the introduction of additional mass and damping elements to the sensor structure, which reduces the quality factor of the diaphragm. The observed larger sensitivity in water is due to the presence of higher pressure level as a result of the denser water environment.

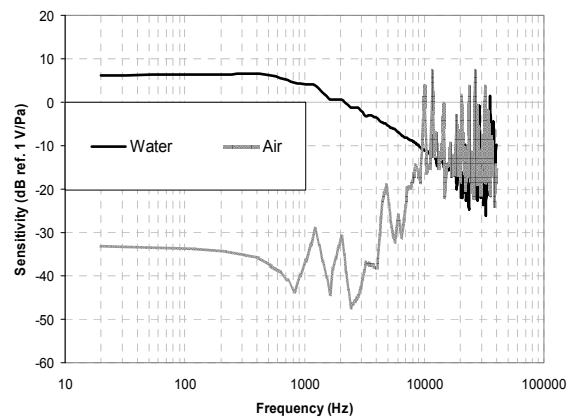


Figure 5: Frequency response of the sensor in air and water.

### Signal Reception

In another underwater experimental setup, the underwater speaker is driven by a 1 kHz sinusoidal signal from the dynamic signal analyzer while the sensor output is captured by Tektronix MSO 4104 Mixed Signal Oscilloscope. Figure 6 illustrates a photograph of the oscilloscope screen that shows the transmitted (signal to speaker) and received (sensor signal) sinusoidal signals in

water at 1 kHz. As illustrated, the input to the underwater speaker (the power amplifier gain is set to unity) is measured to be  $4\text{ V}_{\text{p-p}}$  while the sensor output (the preamplifier gain is set to 10) is measured to be  $0.35\text{ V}_{\text{p-p}}$ .

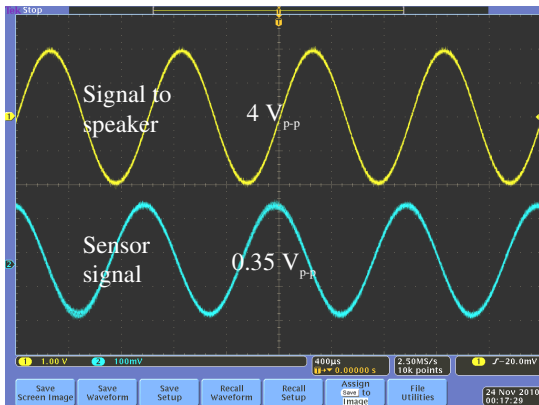


Figure 6: Transmitted (signal to speaker) and received (sensor signal) sinusoidal signals at 1 kHz.

## CONCLUSION

A micromachined piezoelectric diaphragm-based pressure sensor has been fabricated and packaged for underwater applications. Key fabrication steps include a low-temperature bonding technique, PZT layer integration, formation of electrode interconnect and pads, CMP, PZT wet etching and DRIE. For the packaging scheme, LCP and PDMS are used to seal and waterproof the sensor dies and electrical connection. In water, the presence of additional mass and damping elements leads to a damped frequency response as a result of the quality factor reduction of the sensing diaphragm while the observed larger sensitivity can be attributed to the higher pressure level due to the denser water environment.

## ACKNOWLEDGMENTS

This research was funded by the Singapore National Research Foundation (NRF) through the Singapore-MIT Alliance for Research and Technology (SMART) Centre, Center for Environmental Sensing and Modeling (CENSAM) IRG.

## REFERENCES

- [1] C. W. Tan, Z. H. Wang, J. M. Miao and X. F. Chen, "A Study on the Viscous Damping Effect for Diaphragm-Based Acoustic MEMS Applications", *J. Micromech. Microeng.*, Vol. 17, pp. 2253-2263, 2007.
- [2] Z. H. Wang, J. M. Miao and C. W. Tan, "Acoustic Transducers with a Perforated Damping Backplate Based on PZT/Silicon Wafer Bonding Technique", *Sens. Actuators A*, Vol. 149, pp. 277-283, 2009.
- [3] F. X. Ke, J. M. Miao and C. W. Tan, "Performance Enhancement by Substrate Perforation for a Wafer-Level Encapsulated RF MEMS DC Shunt Switch", *Proc. IEEE MEMS 2009 Conference, Sorrento, Italy*, January 25-29, 2009, pp. 876-879.
- [4] M. Olfatnia, Z. Shen, J. M. Miao, L. S. Ong, T. Xu and M. Ebrahimi, "Medium Damping Influences on the Resonant Frequency and Quality Factor of Piezoelectric Circular Microdiaphragm Sensors", *J. Micromech. Microeng.*, Vol. 21, pp. 1-9, 2011.
- [5] Z. H. Wang, J. M. Miao, C. W. Tan and T. Xu, "Fabrication of Piezoelectric MEMS Devices - From Thin Film to Bulk PZT Wafer", *J. Electroceram.*, Vol. 24, pp. 25-32, 2010.
- [6] K. W. Oh, A. Han, S. Bhansali and C. H. Ahn, "A Low-Temperature Bonding Technique Using Spin-On Fluorocarbon Polymers to Assemble Microsystems", *J. Micromech. Microeng.*, Vol. 12, pp. 187-191, 2002.
- [7] K. Zheng, J. Lu and J. Chu, "A Novel Wet Etching Process of  $\text{Pb}(\text{Zr,Ti})\text{O}_3$  Thin Films for Applications in Microelectromechanical System", *Jpn. J. Appl. Phys.*, Vol. 43, pp. 3934-3937, 2004.
- [8] X. Wang, J. Engel and C. Liu, "Liquid Crystal Polymer (LCP) for MEMS: Processes and Applications", *J. Micromech. Microeng.*, Vol. 13, pp. 628-633, 2003.
- [9] H. Lamb, "On the Vibrations of an Elastic Plate in Contact with Water", *Proc. Royal Soc. London A*, Vol. 98, pp. 205-216, 1920.

## CONTACT

\* J.M. Miao, tel: 65-67906038; mjmmiao@ntu.edu.sg